



Anisotropic neutron spin resonance in superconducting $\text{BaFe}_{1.9}\text{Ni}_{0.1}\text{As}_2$

O. J. Lipscombe,^{1,*} Leland W. Harriger,¹ P. G. Freeman,² M. Enderle,² Chenglin Zhang,¹ Miaoying Wang,¹ Takeshi Egami,^{1,3,4} Jiangping Hu,^{5,6} Tao Xiang,^{6,7} M. R. Norman,⁸ and Pengcheng Dai^{1,4,6,†}

¹*Department of Physics and Astronomy, The University of Tennessee, Knoxville, Tennessee 37996-1200, USA*

²*Institut Laue-Langevin, 6, rue Jules Horowitz, BP 156, 38042 Grenoble Cedex 9, France*

³*Department of Materials Science and Engineering, The University of Tennessee, Knoxville, Tennessee 37996-1200, USA*

⁴*Oak Ridge National Laboratory, Oak Ridge, Tennessee 37831, USA*

⁵*Department of Physics, Purdue University, West Lafayette, Indiana 47907, USA*

⁶*Institute of Physics, Chinese Academy of Sciences, Beijing 100190, China*

⁷*Institute of Theoretical Physics, Chinese Academy of Sciences, P.O. Box 2735, Beijing 100190, China*

⁸*Materials Science Division, Argonne National Laboratory, Argonne, Illinois 60439, USA*

(Received 5 March 2010; revised manuscript received 14 July 2010; published 18 August 2010)

We use polarized inelastic neutron scattering to show that the neutron spin resonance below T_c in superconducting $\text{BaFe}_{1.9}\text{Ni}_{0.1}\text{As}_2$ ($T_c=20$ K) is purely magnetic in origin. Our analysis further reveals that the resonance peak near 7 meV only occurs for the planar response. This challenges the common perception that the spin resonance in the pnictides is an isotropic triplet excited state of the singlet Cooper pairs, as our results imply that only the $S_{001}=\pm 1$ components of the triplet are involved.

DOI: [10.1103/PhysRevB.82.064515](https://doi.org/10.1103/PhysRevB.82.064515)

PACS number(s): 74.70.Xa, 75.30.Gw, 78.70.Nx

I. INTRODUCTION

The neutron spin resonance is a collective magnetic excitation appearing in the superconducting state of high-transition temperature (high- T_c) copper oxide superconductors.¹⁻⁴ Since its initial discovery in optimal hole-doped $\text{YBa}_2\text{Cu}_3\text{O}_{6+x}$,¹⁻⁴ the resonance has been found in electron-doped cuprates,⁵ heavy fermion,^{6,7} and iron arsenide superconductors.⁸⁻¹³ Below the superconducting transition temperature T_c , the intensity of the resonance increases like the superconducting order parameter and its energy scales with T_c .⁵ Although the resonance appears to be a ubiquitous property of unconventional superconductors,¹⁻¹² its microscopic origin and relationship with superconductivity are still debated.¹⁴ In all these materials, the resonance occurs at the antiferromagnetic (AF) wave vector \mathbf{Q} of the parent compound. It is thought to be a triplet excitation of the singlet Cooper pairs,^{14,15} implying a superconducting order parameter that satisfies $\Delta_{k+Q}=-\Delta_k$. In the iron arsenide superconductors, this condition is satisfied by an order parameter whose sign reverses between the electron and hole pockets.¹⁶⁻²⁰ If this picture is correct, one would expect that the triplet would be degenerate, and thus directionally isotropic in space. For the optimal hole-doped high- T_c cuprate superconductor $\text{YBa}_2\text{Cu}_3\text{O}_{6+x}$, polarized inelastic neutron-scattering experiments suggest that this is indeed the case.^{2,3}

We report polarized inelastic neutron-scattering results for the optimal electron-doped iron arsenide superconductor $\text{BaFe}_{1.9}\text{Ni}_{0.1}\text{As}_2$ ($T_c=20$ K).^{10,11} We find that the resonance previously observed around 7 meV at the AF wave vector $\mathbf{Q}=(0.5,0.5,1)$ (reciprocal lattice units, “rlu”) is entirely magnetic but displays strong spin-space anisotropy, with a peaked response near the resonance energy occurring only for the planar response. This is different from the momentum space anisotropy, where the spin correlation length might be

different along different crystallographic directions.²¹⁻²³ Our results indicate a strong spin-orbital/lattice coupling in iron arsenide superconductors (quite different from the cuprates), and are a challenge to the common assumption that the resonance represents an isotropic singlet-to-triplet excitation.

II. EXPERIMENTAL DETAILS

A. Sample

We chose the iron arsenide superconductor $\text{BaFe}_{1.9}\text{Ni}_{0.1}\text{As}_2$ because this material has no static AF order [Fig. 1(b)], exhibits a well-defined neutron spin resonance near 7 meV at $\mathbf{Q}=(0.5,0.5,1)$ above a clear spin gap, and is available in large, homogeneous single crystals.^{10,11} We coaligned ~ 5 g of single crystals (with mosaic of 3° full width half maximum) in the (H,H,L) scattering plane,^{10,11} where the wave vector \mathbf{Q} is indexed $\mathbf{Q}=\mathbf{H}\mathbf{a}^*+\mathbf{K}\mathbf{b}^*+\mathbf{L}\mathbf{c}^*$ with $\mathbf{a}^*=\hat{a}2\pi/a$, etc., $a=b=3.93$ Å and $c=12.77$ Å [Fig. 1(a)]. In this tetragonal notation, the AF order and resonance occur at $\mathbf{Q}=(0.5,0.5,L)$ with $L=\pm 1, \pm 3, \dots$ (Refs. 9–11).

B. Polarized neutron analysis

We carried out polarized inelastic neutron-scattering experiments using the Cryopad capability of the IN20 triple-axis spectrometer at the Institut Laue-Langevin, Grenoble, France. Neutron polarization analysis is the only way to conclusively separate the magnetic signal from lattice effects, and to determine the spatial anisotropy of the magnetic excitations.

In principle, polarization analysis can be used to completely separate magnetic (e.g., spin fluctuation) and nuclear (e.g., phonon) scattering because the spin of the neutron is always flipped in a magnetic interaction where the neutron polarization is parallel to the wave-vector transfer \mathbf{Q} .²⁴ For

convenience, we define the neutron polarization directions along \mathbf{Q} as x , perpendicular to \mathbf{Q} but in the scattering plane as y , and perpendicular to \mathbf{Q} and the scattering plane as z , respectively [Fig. 1(c)]. At a specific wave vector and energy, we measured the six cross sections which correspond to the three incoming neutron polarization directions x , y , and z , with the outgoing neutron polarization either parallel to the incoming (neutron nonspin flip or NSF) or antiparallel (neutron spin flip or SF). The measured neutron cross sections are then accordingly written as $\sigma_\alpha^{\text{NSF}}$ and $\sigma_\alpha^{\text{SF}}$, where $\alpha=x,y,z$.²⁴ With the Cryopad setup, these cross sections can be measured with the sample in a strictly zero magnetic field (<10 mG), thus avoiding errors due to flux inclusion or field expulsion in the superconducting phase of the sample.

We define the magnetic intensity of excitations with fluctuating magnetic moments pointing parallel to the (1,1,0) (in-plane) direction as $M(110)$, and the intensity of fluctuating moments pointing out of plane as $M(001)$. Our experiment probes M_y and M_z , the magnetic intensity of excitations with the moment parallel to y and z , respectively [see Fig. 1(c)]. Due to tetragonal symmetry $M(110)=M(1\bar{1}0)\equiv M_z$, and $M(001)$ can be found from M_y using $M_y=M(110)\sin^2\theta+M(001)\cos^2\theta$, where θ is the angle between wave vectors (1,1,0) and \mathbf{Q} [see Fig. 1(d)].

The measured cross section can be written as

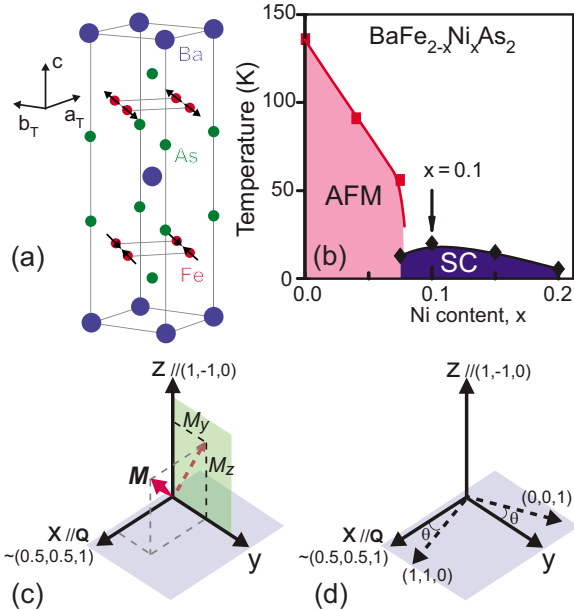


FIG. 1. (Color online) (a) Crystal structure of BaFe₂As₂. (b) Magnetic and superconducting phase diagram of BaFe_{2-x}Ni_xAs₂ with the present composition highlighted with an arrow (Ref. 13). (c) Schematic showing a fluctuating atomic magnetic moment vector \mathbf{m} , and the components m_y and m_z which are probed. Neutron-scattering intensity is related to the square of the fluctuating moment components in the y and z direction, $M_y=\langle m_y^2 \rangle$ and $M_z=\langle m_z^2 \rangle$, respectively (which are both defined perpendicular to x , where x is parallel to the wave vector \mathbf{Q}). (d) Schematic showing crystallographic in-plane (1,1,0), (1,-1,0), and out of plane (0,0,1) directions compared with the x , y , and z directions defined above.

$$\begin{pmatrix} \sigma_x^{\text{SF}} - b_1 \\ \sigma_y^{\text{SF}} - b_1 \\ \sigma_z^{\text{SF}} - b_1 \\ \sigma_x^{\text{NSF}} - b_2 \\ \sigma_y^{\text{NSF}} - b_2 \\ \sigma_z^{\text{NSF}} - b_2 \end{pmatrix} = \frac{1}{R+1} \begin{pmatrix} R & R & 1 \\ 1 & R & 1 \\ R & 1 & 1 \\ 1 & 1 & R \\ R & 1 & R \\ 1 & R & R \end{pmatrix} \begin{pmatrix} M_y \\ M(110) \\ N \end{pmatrix} \quad (1)$$

with a nuclear scattering strength N (containing both phonon and inelastic incoherent nuclear scattering), and b_1 and b_2 account for instrumental background (and nuclear-spin incoherent scattering). R specifies the quality of the neutron beam polarization (so that leakage between SF and NSF channels caused by imperfect polarization are taken into account). In our setup, we measured R by the leakage of nuclear Bragg peaks into the (magnetic) SF channel $R=\sigma_{\text{Bragg}}^{\text{NSF}}/\sigma_{\text{Bragg}}^{\text{SF}}\approx 15$, independent of neutron polarization direction. To extract M_y and $M(110)$ from the raw data, we can use [from Eq. (1)]

$$\sigma_x^{\text{SF}} - \sigma_y^{\text{SF}} = \sigma_y^{\text{NSF}} - \sigma_x^{\text{NSF}} = cM_y,$$

$$\sigma_x^{\text{SF}} - \sigma_z^{\text{SF}} = \sigma_z^{\text{NSF}} - \sigma_x^{\text{NSF}} = cM(110), \quad (2)$$

where $c=(R-1)/(R+1)$. With Eq. (2), we can estimate the energy and wave-vector dependence of $M(110)$ or M_y from a weighted average of the pair of values calculated using the SF and the NSF data.

III. RESULTS

Figures 2(a) and 2(b) show σ_x^{SF} (primarily magnetic) and σ_x^{NSF} (primarily nuclear) energy cuts at (0.5,0.5,1) taken at temperatures of 1.5 K ($\ll T_c$) and 30 K ($> T_c$), respectively. As the temperature decreases, it is clear that the nuclear scattering (σ_x^{NSF}) changes very little with temperature while the magnetic scattering (σ_x^{SF}) around 7 meV is enhanced, and below ~ 3 meV becomes gapped.^{10,11} These data unambiguously demonstrate that the resonance is purely magnetic without any lattice contribution. Figure 2(c) shows a $T=1.5$ K Q cut along the $(H,H,1)$ trajectory at 7 meV [Fig. 2(d)]. Consistent with unpolarized measurements,^{10,11} the data prove that the resonance is magnetic scattering centered at $(H,K)=(0.5,0.5)$.

Having established the magnetic nature of the resonance, we now probe the anisotropy of the spin-fluctuation spectrum by measuring $\sigma_{x,y,z}^{\text{SF}}$ and $\sigma_{x,y,z}^{\text{NSF}}$ and using Eq. (2) to calculate $M(110)$ and $M(001)$. σ_y^{SF} exclusively probes the in-plane spin fluctuations $M(110)$ and σ_z^{SF} gives the intensity of moments fluctuating along $M_y \sim M(001)$. Finally, σ_x^{SF} is the magnetic part of the cross section observed in unpolarized measurements and provides the sum of the magnetic scattering, in this case $M_y+M(110)$. For isotropic paramagnetic spin fluctuations, one expects $M_y=M(110)$ and this appears to be the case for the resonance in optimal doped YBa₂Cu₃O_{6+x}.^{2,3}

Figures 3(a)–3(d) show all six scattering cross sections $\sigma_{x,y,z}^{\text{SF}}$ and $\sigma_{x,y,z}^{\text{NSF}}$ raw data taken at $\mathbf{Q}=(0.5,0.5,1)$ below and above T_c . While the resonance at 7 meV is clearly seen in the σ_x^{SF} data at 1.5 K [Fig. 3(a)], a comparison of σ_y^{SF} and σ_z^{SF}

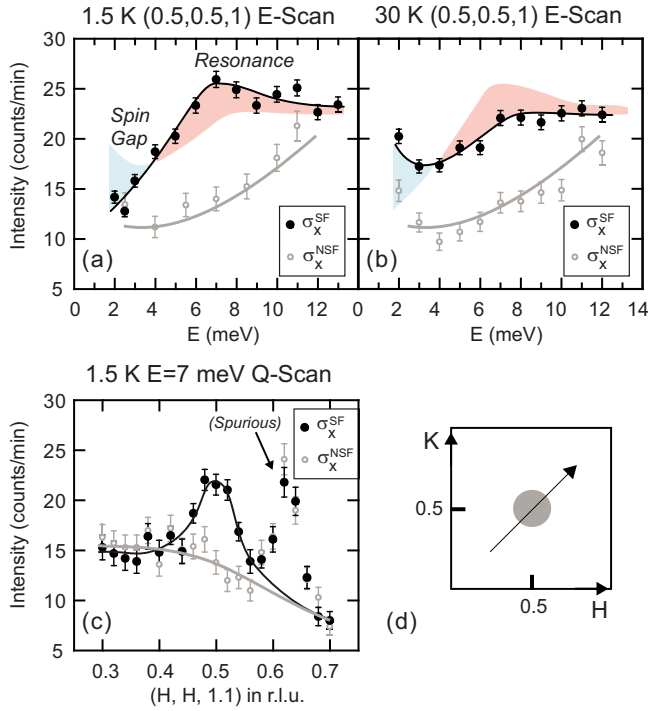


FIG. 2. (Color online) Energy scans at $\mathbf{Q}=(0.5,0.5,1)$, showing σ_x^{SF} (magnetic) and σ_x^{NSF} (nuclear) scattering for (a) 1.5 K and (b) 30 K. (c) $(H, H, 1.1)$ Q scan through the resonance position, showing σ_x^{SF} and σ_x^{NSF} measured at a constant energy 7 meV. The narrow peak at $(0.625, 0.625)$ is temperature-independent spurious scattering. (d) Trajectory in reciprocal space of the $(H, H, 1.1)$ scan. Solid lines are guides to the eyes for all plots except where otherwise stated.

shows that the former has a peak while the latter is featureless near the resonance energy. Since $\sigma_y^{\text{SF}} \sim M(001)$ and $\sigma_y^{\text{SF}} \propto M(110)$, these data immediately suggest anisotropic spin fluctuations near the resonance. By using all six scattering cross sections in Figs. 3(a) and 3(b), we extract the energy dependence of $M(110)$ and $M(001)$ magnetic scattering, and subsequently convert the extracted data to a magnetic response, χ''_{110} and χ''_{001} , [Fig. 3(e)] by dividing out the Bose population factor [also, we can instead extract $M(110)$ and $M(001)$ from only the three SF cross sections, in which case we get quantitatively very similar results]. It is clear that the in-plane response (χ''_{110}) resembles a peak centered at around 7 meV while the out of plane χ''_{001} has a much lower energy scale.

Figures 3(c) and 3(d) show $\sigma_{x,y,z}^{\text{SF}}$ and $\sigma_{x,y,z}^{\text{NSF}}$ measured at 30 K. Compared with the 1.5 K data, the most obvious changes in the $\sigma_{x,y,z}^{\text{SF}}$ data are the suppression of the resonance and the low-energy spin gap. Figure 3(f) plots the energy dependence of the extracted, Bose factor divided $M(110)$ and $M(001)$ at 30 K. In addition to the disappearance of the low-temperature spin gap, it can be seen that χ''_{110} still has a broad peak near $E=7$ meV while χ''_{001} is again relatively featureless. Comparison of the Figs. 3(e) and 3(f) reveals clear evidence for the resonance peak at 7 meV above a spin gap of ~ 3 meV in χ''_{110} while χ''_{001} is featureless near 7 meV with a spin gap of $E \leq 2$ meV.^{10,11} Previous unpolarized neutron-scattering measurements found a spin-gap value of about 3

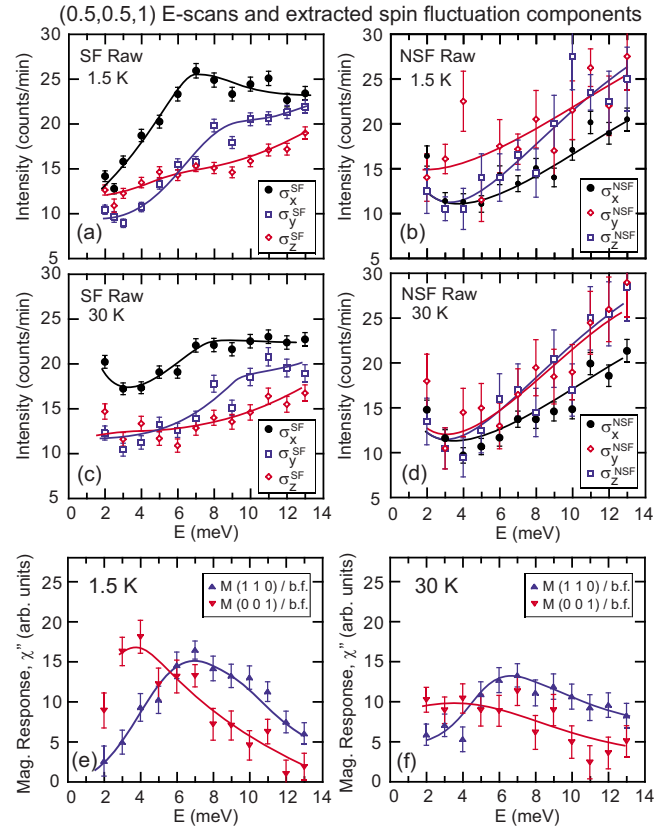


FIG. 3. (Color online) Energy scans at $\mathbf{Q}=(0.5,0.5,1)$. Raw (a) 1.5 K $\sigma_{x,y,z}^{\text{SF}}$ and (b) 1.5 K $\sigma_{x,y,z}^{\text{NSF}}$ cross-section data. Clear anisotropy is evident because $\sigma_y^{\text{SF}} \neq \sigma_z^{\text{SF}}$ and $\sigma_y^{\text{NSF}} \neq \sigma_z^{\text{NSF}}$. (c) and (d) Raw data taken at 30 K. (e) and (f) In-plane and out-of-plane magnetic response [the extracted $M(110)$ and $M(001)$ using raw data in Eq. (2), divided by the Bose factor (b.f.)] at 1.5 K and 30 K, respectively. Data in (e) and (f) are also corrected for second-order monitor overcounting.

meV at $\mathbf{Q}=(0.5,0.5,1)$.¹¹ Our polarized data are consistent with this as well as the unpolarized results²⁵ on the same sample if we combine the extracted $M(110)$ and $M(001)$ results (See Appendix B).

To further understand the anisotropy of the spin fluctuations, we carried out constant-energy scans with all three $\sigma_{x,y,z}^{\text{SF}}$ components at $E=2.5, 7,$ and 11 meV [Figs. 4(a)–4(c)]. At 2.5 meV, below the spin gap, there is a peak at the in-plane wave vector $(0.5, 0.5)$ in $\sigma_z^{\text{SF}} \sim M(001)$ whereas for the identical scan $\sigma_y^{\text{SF}} \propto M(110)$ is featureless. At low \mathbf{Q} ($H \leq 0.4$) at 2.5 meV, the scattering for σ_x^{SF} and σ_z^{SF} have different backgrounds (see Appendix A). This problem is not present in the energy scans or other Q scans taken, where the backgrounds b_1 and b_2 must be independent of polarization direction. These constant- E scans are consistent with the constant- Q scans in Fig. 3(e), suggesting that the spin gap in $M(110)$ is larger than that in $M(001)$. At 7 meV, there are peaks in both channels at $(0.5, 0.5)$ but the anisotropy appears to reverse, implying higher intensity in the in-plane $M(110)$ direction. Similar data are also found for Q scans at 11 meV [Fig. 4(c)], consistent with the constant- Q data in Fig. 3. Finally, we plot in Fig. 4(d) the L dependence of the $\sigma_{x,y}^{\text{SF}}$ scattering at 7 meV and 30 K. Instead of simply falling off as

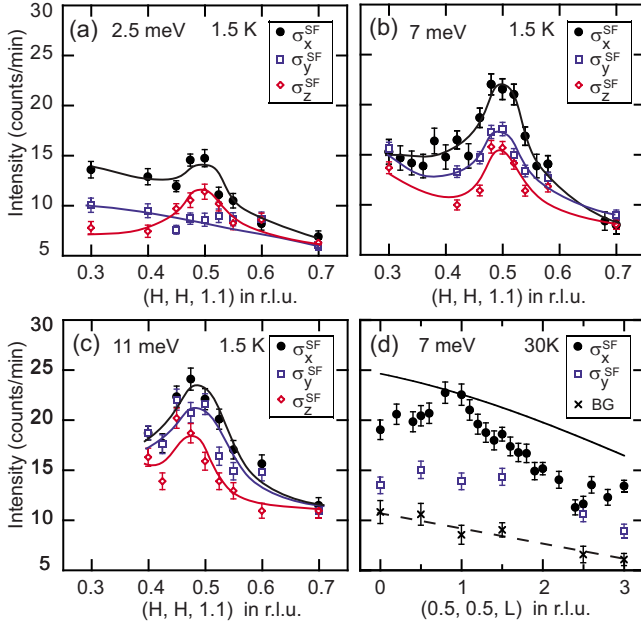


FIG. 4. (Color online) (a)–(c) Q Scans along the $(H, H, 1.1)$ direction at 2.5, 7, and 11 meV, respectively, with all three spin flip cross sections measured. (d) L scan at the resonance energy. Crosses resemble estimated instrumental background points, extracted from the data shown and $\sigma_{x,y}^{\text{NSF}}$ (not shown) using Eq. (1) (assuming $b_1 \approx b_2$). The solid line shows the expected magnetic scattering assuming an Fe^{2+} form factor.

the Fe^{2+} magnetic form factor,^{26,27} σ_x^{SF} peaks near $L=1$ and decreases rapidly with increasing L above the nonmagnetic background. These results suggest that the resonance in $\text{BaFe}_{1.9}\text{Ni}_{0.1}\text{As}_2$ has c -axis modulations similar to underdoped $\text{BaFe}_{2-x}\text{Ni}_x\text{As}_2$ (Ref. 13) and is not entirely two dimensional as in $\text{BaFe}_{1.84}\text{Co}_{0.16}\text{As}_2$.⁹

IV. CONCLUSION

We have performed inelastic neutron measurements with full neutron polarization analysis to measure the magnetic anisotropy of the spin fluctuations in optimally doped superconducting $\text{BaFe}_{1.9}\text{Ni}_{0.1}\text{As}_2$. We have observed the magnetic response of the iron spins pointing along in-plane [parallel to $(1,1,0)$] and out of plane [parallel to $(0,0,1)$] directions to have very different energy dependence. For the in-plane response, the resonance peak was present whereas the out of plane response was reasonably featureless around the resonance energy at 7 meV.

Spin-space anisotropy in the zero energy limit has previously been reported from NMR data on an underdoped hole-doped composition with no magnetic order,²⁸ which can be explained in terms of the proximity of the composition to the ordered parent compound. However, in our nonmagnetically ordered sample, we see not just low-frequency anisotropy but a high-frequency novel response that has different energy dependencies between different spin directions.

The presence of spin-orbital/lattice coupling could explain anisotropy in the spin excitations. In pnictides, this is reflected in the undoped compound, where the moments are

locked to the orthorhombic a axis^{29–31} [along $(1,1,0)$ direction in our tetragonal notation]. The existence of the resonance solely in the in-plane response is a major challenge to the standard theory where the resonance is an isotropic triplet excitation of the singlet superconducting ground state. To understand the origin of our results within the context of this theory,¹⁵ we note that the spin operators \hat{S}_{110} and $\hat{S}_{1\bar{1}0}$, when acting on the spin-singlet superconducting ground state, generate the $S_{001} = \pm 1$ components of the triplet whereas the spin operator \hat{S}_{001} generates the $S_{001} = 0$ component. Our results therefore imply that the resonance is the $S_{001} = \pm 1$ doublet. To understand this microscopically, we note that in the magnetically ordered phase, the $S_{110} = 0$ component of the triplet would mix with the singlet ground state (since the moments are oriented along the orthorhombic a axis). In the nonmagnetic tetragonal state, this would lead to a low-energy doublet $S_{110} = 0$, $S_{1\bar{1}0} = 0$, which is equivalent to $S_{001} = \pm 1$ (see Appendix C). An alternate possibility is that the resonance is instead a magnonlike excitation that becomes undamped because of the opening of the superconducting gap,^{32,33} though it is not clear to us why this scenario would generate a magnetic response that is localized at a particular energy.

ACKNOWLEDGMENTS

The work at UT/ORNL is supported by the U.S. DOE BES No. DE-FG02-05ER46202, and by the U.S. DOE, Division of Scientific User Facilities. Work at IOP is supported by the CAS. Work at ANL is supported by the U.S. DOE under Contract No. DE-AC02-06CH11357. O.J.L. and T.E. were supported by the DOE BES EPSCoR Grant No. DE-FG02-08ER46528.

APPENDIX A: NEUTRON-POLARIZATION-INDEPENDENT BACKGROUNDS AND THE 2.5 meV Q CUT

As implied by Eq. (1) of the paper, in principle, the background scattering into the detector should be the same with neutron polarization in x , y , and z for any given SF (or NSF) measurements since the axes of the instrument do not move. However, there is a moving part that does change with neutron polarization direction, and that is the “dipole magnet” in the outgoing beam, which rotates around the scattered beam axis (with a position depending on polarization direction, as well as Q and E) and creates the neutron guide field that defines the neutron polarization direction. The problem occurs when a choice of Q and E conspires to cause both a scattering angle that is small, and a dipole magnet position close to the horizontal for a certain neutron polarization direction. Neutrons can then scatter in grazing incidence from the dipole magnet shielding, which can increase the background in the detector for that configuration over other neutron polarization directions.

At low Q ($H \leq 0.4$) at $E = 2.5$ meV, these problematic conditions are satisfied creating an extra background in the $\sigma_x^{\text{NSF,SF}}$ configurations. However, the dipole magnet is away from horizontal at the same energy and wave vector for the

$\sigma_y^{\text{NSF,SF}}$ and $\sigma_z^{\text{NSF,SF}}$ configurations, which therefore have lower backgrounds. At higher energies (and other wave vectors), the dipole magnet is never close to horizontal when the scattering angle is small enough for a grazing incidence to reach the detector, and so there is no difference between backgrounds of different neutron polarization configurations. We have confirmed that this is indeed the case, by comparing backgrounds extracted for all the data collected, and found an anomalous effect only for the low \mathbf{Q} region at 2.5 meV.

In conclusion, at $H \leq 0.4$ in the 2.5 meV Q scan there may be a difference between backgrounds in configurations with different neutron polarizations [and thus, in this case the assumption in Eq. (1) may not be valid]. However, this is not a problem in any other scans, and most importantly does not affect the energy scans at any point. Therefore, as required to correctly extract $M(110)$ and $M(001)$, the assumption that the background is neutron polarization direction independent is a good one for the energy scans.

APPENDIX B: COMPARISON OF EXTRACTED DATA AND PREVIOUS UNPOLARIZED RESULTS

From the present study, from observing the two different spin gaps at 3 meV and ≤ 2 meV, and different maxima at approximately 7 and 3 meV in the $M(110)$ and $M(001)$ channels, one might expect to see these features in unpolarized data. The same compound has been previously studied²⁵ by unpolarized neutrons in the $(H, K, 0)$ scattering plane (different from the scattering plane in the present study). Although there is a resonance at 7 meV and a spin gap around 3 meV, the dynamic susceptibility does not have a peak near 3 meV. Here we show that these results are entirely consistent with the present polarized neutron-scattering results.

In the unpolarized experiment, the magnetic scattering measured at $(0.5, 0.5, 0)$ is proportional to $M(110) + M(001)$ for the crystal alignment used. If we assume minimal L dispersion, then we can take the $M(110)$ and $M(001)$ values from our present study (where $L=1$) and simulate the ($L=0$) unpolarized data with no unknown parameters. We can then compare our simulation with the experimental data from the unpolarized experiment. As can be seen from Fig. 5, the low-energy features in $M(001)$ near 3 meV do not cause low energy features in the total unpolarized intensity $M(110) + M(001)$. The resulting form of Fig. 5 is consistent with the data in unpolarized measurements (in Ref. 25), though the resolution in the unpolarized experiment was much better, leading to a much sharper resonance in that study.

APPENDIX C: ORIGIN OF THE DOUBLET RESONANCE

The spin-singlet Cooper-pair wave function is a product of states of the form

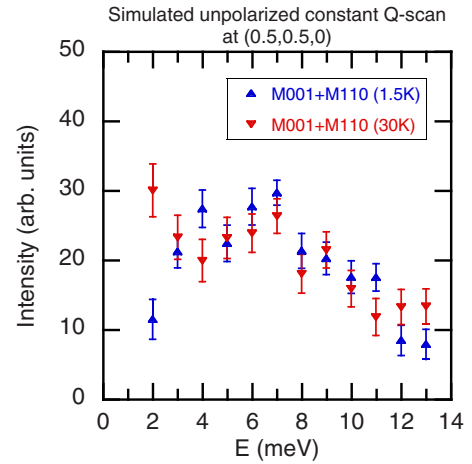


FIG. 5. (Color online) Intensity expected for energy scans at $(0.5, 0.5, 0)$ for an unpolarized experiment, calculated using $M(110)$ and $M(001)$ from the present polarized data.

$$|\Psi_k\rangle = |k\uparrow, -k\downarrow\rangle - |k\downarrow, -k\uparrow\rangle. \quad (\text{C1})$$

We operate on this state with the spin operator, \hat{S} , which is the sum of \hat{S}_1 and \hat{S}_2 where 1 and 2 denote the two electrons of the pair. For the spin raising operator, we find

$$\hat{S}_+(q)|\Psi_k\rangle = |k\uparrow, -k+q\uparrow\rangle - |k+q\uparrow, -k\uparrow\rangle. \quad (\text{C2})$$

This is the $S_z=1$ component of a triplet pair with center of mass momentum q (the minus sign being a reflection of fermion antisymmetry). Similarly, \hat{S}_- generates the $S_z=-1$ component. Had we operated with \hat{S}_z instead, we would have obtained the $S_z=0$ component of the triplet. Therefore, for a quantization axis along c , χ_{aa} , and χ_{bb} generate the $S_c = \pm 1$ doublet whereas χ_{cc} generates the $S_c=0$ state. Since we find no resonance response for χ_{cc} , the resonance is the $S_c = \pm 1$ doublet. To better appreciate this result, assume that superconductivity and antiferromagnetism coexist, corresponding to the spin resonance being at zero energy. If one pairs electrons using antiferromagnetic eigenstates, and then rewrites these pairs in terms of paramagnetic eigenstates, the resulting pair state is well known to be a mixture of a singlet and the $S_z=0$ component of a triplet,³⁴ with z parallel to the direction of the Neel vector. In the isotropic case, the Neel vector can point in any direction, which is why the resonance is a triplet. But for the antiferromagnetic ground state of the pnictides, the spins are locked to the orthorhombic a axis. Therefore, the mixed triplet component of the pairs for a coexisting state would be $S_a=0$. If we then average in the plane so as to restore tetragonal symmetry, then the $S_b=0$ component would be involved as well. Thus we obtain a doublet. If we now rotate the quantization axis to be along the c direction, this doublet corresponds to $S_c = \pm 1$.

*lipscombe@utk.edu

†daip@ornl.gov

- ¹J. Rossat-Mignod, L. P. Regnault, C. Vettier, P. Bourges, P. Burllet, J. Bossy, J. Y. Henry, and G. Lapertot, *Physica C* **185**, 86 (1991).
- ²H. A. Mook, M. Yethiraj, G. Aeppli, T. E. Mason, and T. Armstrong, *Phys. Rev. Lett.* **70**, 3490 (1993).
- ³H. F. Fong, B. Keimer, D. Reznik, D. L. Milius, and I. A. Aksay, *Phys. Rev. B* **54**, 6708 (1996).
- ⁴P. Dai, H. A. Mook, R. D. Hunt, and F. Doğan, *Phys. Rev. B* **63**, 054525 (2001).
- ⁵S. D. Wilson, P. Dai, S. Li, S. Chi, H. J. Kang, and J. W. Lynn, *Nature (London)* **442**, 59 (2006).
- ⁶N. Metoki, Y. Haga, Y. Koike, and Y. Ōnuki, *Phys. Rev. Lett.* **80**, 5417 (1998).
- ⁷C. Stock, C. Broholm, J. Hudis, H. J. Kang, and C. Petrovic, *Phys. Rev. Lett.* **100**, 087001 (2008).
- ⁸A. D. Christianson, E. A. Goremychkin, R. Osborn, S. Rosenkranz, M. D. Lumsden, C. D. Malliakas, I. S. Todorov, H. Claus, D. Y. Chung, M. G. Kanatzidis, R. I. Bewley, and T. Guidi, *Nature (London)* **456**, 930 (2008).
- ⁹M. D. Lumsden, A. D. Christianson, D. Parshall, M. B. Stone, S. E. Nagler, G. J. MacDougall, H. A. Mook, K. Lokshin, T. Egami, D. L. Abernathy, E. A. Goremychkin, R. Osborn, M. A. McGuire, A. S. Sefat, R. Jin, B. C. Sales, and D. Mandrus, *Phys. Rev. Lett.* **102**, 107005 (2009).
- ¹⁰S. Chi, A. Schneidewind, J. Zhao, L. W. Harriger, L. Li, Y. Luo, G. Cao, Z. Xu, M. Loewenhaupt, J. Hu, and P. Dai, *Phys. Rev. Lett.* **102**, 107006 (2009).
- ¹¹S. Li, Y. Chen, S. Chang, J. W. Lynn, L. Li, Y. Luo, G. Cao, Z. Xu, and P. Dai, *Phys. Rev. B* **79**, 174527 (2009).
- ¹²D. S. Inosov, J. T. Park, P. Bourges, D. L. Sun, Y. Sidis, A. Schneidewind, K. Hradil, D. Haug, C. T. Lin, B. Keimer, and V. Hinkov, *Nat. Phys.* **6**, 178 (2010).
- ¹³M. Wang, H. Luo, J. Zhao, C. Zhang, M. Wang, K. Marty, S. Chi, J. W. Lynn, A. Schneidewind, S. Li, and P. Dai, *Phys. Rev. B* **81**, 174524 (2010).
- ¹⁴M. Eschrig, *Adv. Phys.* **55**, 47 (2006).
- ¹⁵E. Demler, W. Hanke, and S.-C. Zhang, *Rev. Mod. Phys.* **76**, 909 (2004).
- ¹⁶I. I. Mazin, D. J. Singh, M. D. Johannes, and M. H. Du, *Phys. Rev. Lett.* **101**, 057003 (2008).
- ¹⁷M. M. Korshunov and I. Eremin, *Phys. Rev. B* **78**, 140509(R) (2008).
- ¹⁸T. A. Maier and D. J. Scalapino, *Phys. Rev. B* **78**, 020514(R) (2008).
- ¹⁹T. A. Maier, S. Graser, D. J. Scalapino, and P. Hirschfeld, *Phys. Rev. B* **79**, 134520 (2009).
- ²⁰K. Seo, C. Fang, B. A. Bernevig, and J. Hu, *Phys. Rev. B* **79**, 235207 (2009).
- ²¹C. Lester, J. H. Chu, J. G. Analytis, T. G. Perring, I. R. Fisher, and S. M. Hayden, *Phys. Rev. B* **81**, 064505 (2010).
- ²²S. O. Diallo, D. K. Pratt, R. M. Fernandes, W. Tian, J. L. Zarestky, M. Lumsden, T. G. Perring, C. L. Broholm, N. Ni, S. L. Bud'ko, P. C. Canfield, H.-F. Li, D. Vaknin, A. Kreyssig, A. I. Goldman, and R. J. McQueeney, *Phys. Rev. B* **81**, 214407 (2010).
- ²³H. Li, C. Broholm, D. Vaknin, R. Fernandes, D. Abernathy, M. Stone, D. Pratt, W. Tian, Y. Qiu, N. Ni, S. Diallo, J. Zarestsky, S. Bud'ko, P. Canfield, and R. McQueeney, [arXiv:1003.1687](https://arxiv.org/abs/1003.1687) (unpublished).
- ²⁴R. M. Moon, T. Riste, and W. C. Koehler, *Phys. Rev.* **181**, 920 (1969).
- ²⁵J. Zhao, L.-P. Regnault, C. Zhang, M. Wang, Z. Li, F. Zhou, Z. Zhao, C. Fang, J. Hu, and P. Dai, *Phys. Rev. B* **81**, 180505(R) (2010).
- ²⁶Y. Lee, D. Vaknin, H. F. Li, W. Tian, J. L. Zarestky, N. Ni, S. L. Bud'ko, P. C. Canfield, R. J. McQueeney, and B. N. Harmon, *Phys. Rev. B* **81**, 060406(R) (2010).
- ²⁷W. Ratcliff, P. A. Kienzle, J. W. Lynn, S. Li, P. Dai, G. F. Chen, and N. L. Wang, *Phys. Rev. B* **81**, 140502(R) (2010).
- ²⁸K. Matano, Z. Li, G. L. Sun, C. T. Lin, M. Ichioka, and G. Zheng, *EPL* **87**, 27012 (2009).
- ²⁹Q. Huang, Y. Qiu, W. Bao, M. A. Green, J. W. Lynn, Y. C. Gasparovic, T. Wu, G. Wu, and X. H. Chen, *Phys. Rev. Lett.* **101**, 257003 (2008).
- ³⁰J. Zhao, W. Ratcliff, J. W. Lynn, G. F. Chen, J. L. Luo, N. L. Wang, J. Hu, and P. Dai, *Phys. Rev. B* **78**, 140504(R) (2008).
- ³¹A. I. Goldman, D. N. Argyriou, B. Ouladdiaf, T. Chatterji, A. Kreyssig, S. Nandi, N. Ni, S. L. Bud'ko, P. C. Canfield, and R. J. McQueeney, *Phys. Rev. B* **78**, 100506(R) (2008).
- ³²D. K. Morr and D. Pines, *Phys. Rev. Lett.* **81**, 1086 (1998).
- ³³A. V. Chubukov and L. P. Gor'kov, *Phys. Rev. Lett.* **101**, 147004 (2008).
- ³⁴E. W. Fenton, *Prog. Theor. Phys.* **80**, 94 (1984).